

Utilization of natural clay for retention of some radionuclides: Kinetic and modeling study

S. I. Moussa, M. Holial and R. R. Sheha

Nuclear Chemistry Department, Hot Laboratories Center,
Atomic Energy Authority, P. No. 13759, Cairo, Egypt.

استخدام طين طبيعي لإحتباس بعض العناصر المشعة : دراسة الحركية والنمذجة

صابر موسى ، محمد هليل ، رضا شحبه
قسم الكيمياء النووية - مركز المعامل الحارة - هيئة الطاقة الذرية- مصر

المخلص

في هذا البحث تم تجميع عينة تربة من البيئة المحيطة بهيئة الطاقة الذرية المصرية و استخدمت في دراسة السلوك الامتصاصي لعنصري السيزيوم و الايروبيوم من المحاليل المائية. و تم توصيف الخواص المعدنية و الطبيعية للتربة باستخدام كلا من حيود الأشعة السينية و الأشعة تحت الحمراء و XRF. و بينت النتائج ان عينة التربة لديها سلوك امتصاصي كبير ، و قدرة رائعة في التفاعلات التبادلية مع العديد من ايونات المعادن. وكانت قيم التركيز الكلي للمجموعات الوظيفية الحمضية في سطحها هي 110 مل مكافئ / 100 جم ، بينما بلغ تركيز الجماعات الوظيفية القاعدية إلى 40 مل مكافئ / 100 جم. و تبين النتائج ان إحتباس السيزيوم و الايروبيوم هو عملية عكسية ، و ان عينة التربة لها إمكانات جيدة للاحتفاظ بكلا العنصرين. و اوضحت النتائج ان امتصاصهذين العنصرين يتبع تفاعلات الرتبة الثانية و يبدي قيما لكلا من Q_2 و K_2 مقدارها 3.86 مجم/جم و 3.95×10^{-2} مجم/جم دقيقة لإحتباس السيزيوم ، في حين كانت قيمتها لإحتباس الايروبيوم هي 4.01 مجم/جم و 5.22×10^{-2} مجم/جم دقيقة على التوالي.

Abstract

In this work, a clay sample was collected from a shallow land around Egyptian AEA and applied to investigate the sorption behavior of Cs(I) and Eu(III) from aqueous solution. The mineralogical and physicochemical properties of the clay were characterized. XRD findings and FR-IR spectra evidences with XRF determinations indicate that the clay sample has a significant sorption behavior and remarkable exchange interactions with many metal ions. Retention of Cs and Eu is a reversible process and the applied clay has a good potential for retention of both metal ions. The sorption reaction

was estimated to be second-order kinetic with q_2 and k_2 values of 3.86 mg.g^{-1} and $3.95 \times 10^{-2} \text{ g.mg}^{-1}.\text{min}^{-1}$ for cesium retention on the clay while their values for europium retention were 4.01 mg.g^{-1} and $5.22 \times 10^{-2} \text{ g.mg}^{-1}.\text{min}^{-1}$, respectively. The results indicate that the intraparticle diffusion model fits the experimental data for an initial period of the sorption process.

Introduction

The radioactive contamination has become a crucial public health, safety, and environmental issue. Even trace amounts of radionuclides can be enough to cause concern [1]. Nowadays, the management of radioactive waste is an issue of concern to the public. The complexity of radioactive waste management is one of the most significant challenges faced by all countries. In particular, disposal of such waste in deep underground-geological repositories has become an effective and universally preferred option which is a safety method to avoid the radioactive waste releasing to biosphere environment [2]. The sorption of radioactive elements on mineral surfaces along potential migration paths is an important process in retarding their ultimate transport in the aqueous phase, and as such plays a significant role in environmental safety assessment studies of geological radioactive repositories [3]. Therefore, investigation regarding interaction mechanism of radionuclides at water–solid interface plays a vital role in evaluating fate and transport of radionuclides in geological repository [4-5].

Soil is one of the key elements for all terrestrial ecosystems. It is a very complex heterogeneous medium, which consists of solid phases (the soil matrix) containing minerals and organic matter, and fluid phases (the soil water and the soil air), which interact with each other and ions entering the soil system. The ability of soils to sorb metal ions from aqueous solution is of special interest and has consequences for remediation of polluted soils and waste deposition [6].

Cesium is an alkali element ($Z = 55$) that has high solubility in water. It possesses several radioactive isotopes, the most important of which are ^{134}Cs ($t_{1/2} = 2.06$ years), ^{135}Cs ($t_{1/2} = 3.0 \times 10^6$ years), and ^{137}Cs ($t_{1/2} = 30.17$ years) produced during nuclear fission processes. The fission yields of ^{135}Cs and ^{137}Cs are relatively high, 6.54 and 6.18 %, respectively [7]. Due to their long half-lives, both of ^{135}Cs and ^{137}Cs are principal radiocontaminants. Cs^+ ion can be highly mobile in aqueous media due to its low hydration energy (-276 kJ/mol) as

compared to elements of larger oxidation state or smaller size, for which the hydration energies can rise up to several thousands of kilojoules per mole. This property facilitates its involvement with the hydrological cycle, which has interfaces with the biological cycle and thus poses a potential detriment to man and to other living systems.

Europium is a trivalent lanthanide and a chemical homologue of trivalent actinides as both trivalent lanthanides and actinides exhibit similar sorption properties [8]. Many researchers investigated the sorption of Eu(III) from aqueous solutions as a function of pH, ionic strength, temperature and solution concentrations by a variety of adsorbents such as metal hydroxides [9-10] and clay minerals [11-12].

In this work, the sorption behavior of Cs(II) and Eu(III) onto the proposed soil was investigated to assess its retainability and efficiency removal of Cs^+ and Eu^{3+} from aqueous waste solutions. The mineralogical and physicochemical properties of the soil were characterized and a kinetic study was performed.

Experimental

Materials

All reagents and chemicals used were of analytical grade and the aqueous solutions were prepared using double distilled water. The clay sample was collected from a shallow land around the Atomic Energy Authority, Arab Republic of Egypt. The sample was left to air dry at room temperature, then crushed and sieved at a mesh size lower than 200 μm . The radioactive tracers (Cs and Eu) were locally prepared by neutron irradiation. In this concern, a suitable weight of each target material was wrapped in an aluminum foil and irradiated in the Egyptian second research reactor. After cooling, the samples were dissolved in appropriate solvents, evaporated to dryness and redissolved in double distilled water. The radionuclides activity was γ -radiometrically assayed using a well type NaI scintillation crystal connected to a single channel analyzer model 5000, Oxford, USA.

Clay Characterization

The specific surface area was measured by the BET-N₂ method using a Micrometrics surface area analyzer model ASAP 2010. The surface characteristics were characterized by Fourier Transform Infrared (FTIR) spectrophotometer Nicolet iS10, Thermo, USA. The

elemental composition of the clay sample, as oxide percentages, was determined by x-ray fluorescence technique using Philips PW-2400 Sequential x-ray spectrometer. In order to identify the principal minerals present, an x-ray diffractometric analysis was carried out using Shimadzu XD1180 x-ray diffractometer. The surface morphology of the samples was characterized using a scanning electron microscope (SEM) model JSM-6510 LA from JOEL, Japan. The pH point of zero charge (pH_{pzc}), major exchangeable elements and cation exchange capacity (CEC) were determined using the standard methods [13].

Sorption Procedure

Sorption experiments were performed, using a batch technique, by equilibrating 0.1g of clay sample with a certain volume of solution traced with a prefixed initial activity of ^{134}Cs or $^{152+154}\text{Eu}$ in sealed glass bottles. The samples were shaken at room temperature using a thermostated water bath shaker of Stuart Scientific SBS-30 type, UK. Aliquots were taken at appropriate time intervals as necessary, centrifuged and the radionuclides activity was γ -radiometrically assayed. The pH values were adjusted with 0.1M HCl and/or 0.1M NaOH solutions using MA-235 digital pH meter from Mettler Toledo, UK. All experimental data were the average of three replications of each experiment and the reproducibility of experimental measurements were mostly within $\pm 3\%$. The performed work was done at room temperature ($26 \pm 1\text{ }^\circ\text{C}$) and $V/m = 100\text{ mLg}^{-1}$.

Results and Discussion

3.1. Characterization of the sample

The infrared spectrum of the clay sample is shown in Fig. 1. The spectrum exhibits different bands obviously characteristic to the vibration motion of the different metal oxides that present as main constituents in the clay sample. The broad absorption band observed at 3619 cm^{-1} may be related to OH stretching vibration present in the group Al–OH–Al. The bands detected at 3429 and 1653 cm^{-1} may be revealed to the stretching vibration and deformation of OH of water, respectively. The bending and stretching vibrations of the tetrahedron of the group Si–O exhibited a strong band at 1036 cm^{-1} . The characteristic peak for the stretching vibration of C–H was observed at 1421 cm^{-1} and could be assigned to $\nu_s(\text{C-H})$ [14]. Generally, the bands arising in the

low wavenumber region are corresponded the vibration characteristics of M–O bonding [15].

Figure 2 illustrates the XRD pattern of clay sample. The data clarified that the clay sample can be considered as a multi-component system has main mineral composition of quartz, smectite, kaolinite, calcite, feldspar and gypsum. The main chemical composition of the clay sample was determined using XRF spectroscopy and data are presented in Table 1. It shows that the clay is essentially made up of SiO₂ (56.98 wt %), Al₂O₃ (17.52 wt %) and Fe₂O₃ (7.64 w %) in addition to calcium, magnesium, titanium and other trace oxides.

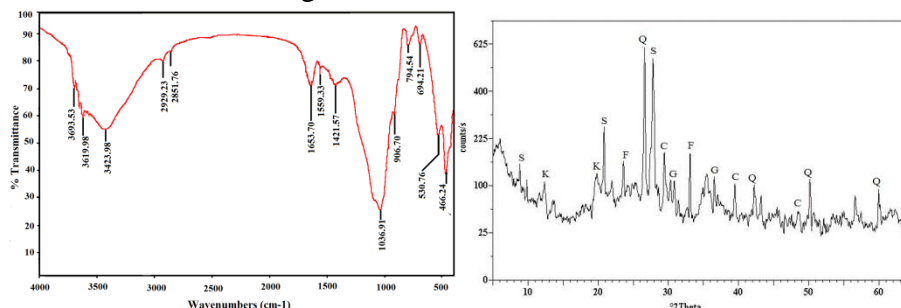


Fig. 1: FT-IR of the clay sample. Fig. 2: XRD of clay sample.

These oxides play extremely important roles in the chemistry of soil. Moreover, the similarity and coincidence of XRD findings and FR-IR spectra evidences with XRF determinations indicates that the clay sample has a significant sorption behavior and remarkable exchange interactions with many metal ions.

Table 1. Main chemical composition of the clay sample.

Analyte	Formula	Wt.%	Analyte	Formula	Wt. %
Si	SiO ₂	56.98	K	K ₂ O	0.85
Al	Al ₂ O ₃	17.52	P	P ₂ O ₅	0.37
Fe	Fe ₂ O ₃	7.64	Ti	TiO ₂	1.47
Mn	MnO	0.18	S	SO ₃	0.34
Ca	CaO	5.27	Cr	Cr ₂ O ₃	0.03
Na	Na ₂ O	0.73	Sr	SrO	0.02
Mg	MgO	2.52	Zr	ZrO ₂	0.02

The average content of the exchangeable elements were determined using H₂O and 0.05 M HCl as eluents and data are given in Table 2. In bi-distilled medium, considerable concentrations of Na⁺, K⁺ and Ca²⁺ are released from the clay samples as well as trace amount of many other elements. The highly exchanged elements are Ca²⁺ and Na⁺. Equilibration of the clay sample in slightly acidic medium of HCl resulted in a release of Si⁴⁺, Al³⁺, Ca²⁺ and Na⁺ beside minor amounts of other ions. Among these elements, Si⁴⁺ and Al³⁺ are the highest exchanged cations. All these exchanged cations report the high exchange capacity of the clay and highlight its ability to be effectively used in retention of different radionuclides.

Table 2. The exchangeable elements content of the clay sample.

No	Exchangeable cations	Concentration (g.kg ⁻¹)	
		H ₂ O	0.05 M HCl
1	K ⁺	5.29	7.65
2	Na ⁺	23.58	29.13
3	Ca ²⁺	36.75	40.06
4	Sr ²⁺	0.55	6.51
5	Mn ²⁺	0.46	12.12
6	Mg ²⁺	2.20	2.67
7	Fe ³⁺	0.05	10.86
8	Cr ⁴⁺	0.07	0.11
9	Al ³⁺	0.72	38.17
10	Si ⁴⁺	7.48	86.46
Sum of exchangeable cations (CEC)		77.15	233.74

The pH corresponding to a solid surface charge of zero is presented in Fig. 3. As seen, the titration curve had a classic sigmoidal shape. The plots showed a large pH changes with acid or base additions, indicating that the clay sample appreciably exhibits amphoteric properties.

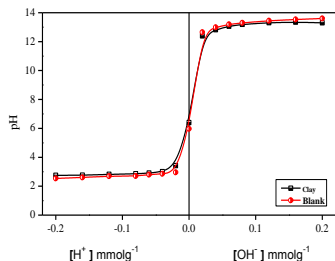


Fig. (3) The titration curve of the clay sample at $I = 0.1 \text{ M}$, $V/m = 100$, $\text{temp} = 24 \pm 1 \text{ }^\circ\text{C}$, $\text{time} = 48 \text{ h}$.

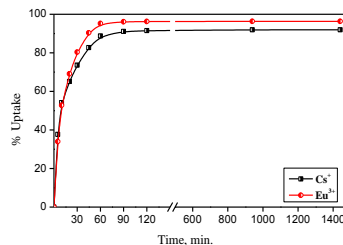


Fig. (4) Variation of removal percent as a function of time for Cs(I) and Eu(III) retention onto clay.

Hence, at solution pH above the pH_{pzc} , the clay surface charge will be negative and favor the sorption of cations while at pH below the pH_{pzc} , the sorption of anions occur [16]. In addition, other physicochemical characteristics of the applied clay were determined using different techniques and the results are given in Table 3. The specific surface area, measured by the N_2 -BET method was found $21.41 \text{ m}^2 \cdot \text{g}^{-1}$. This high value, compared with other clays, reveals the existence of a high porosity responsible for the strong capacity of this material to fix some cations.

3.2. Kinetic study

3.2.1. Contact time

Contact time is studied to optimize the equilibrium time for the sorption of Cs(I) and Eu(III) onto the clay sample. The experiment was carried out keeping the initial concentration at 40 mg/L for both elements. The removal of Cs(I) as well as Eu(III) by this clay at definite time intervals is depicted in Fig. 4. Figure clearly demonstrates that a fast initial uptake was occurred which further slowed down with the lapse of time and an apparent equilibrium is achieved within 60 min of contact time.

Table 3. Physicochemical characteristics of the clay sample.

Property	Result	Comment
Specific surface area ($\text{m}^2 \cdot \text{g}^{-1}$)	21.41	BET
Pore volume ($\text{cm}^3 \cdot \text{g}^{-1}$)	5.36 e^{-2}	N_2 ads.
Acidic surface FG ($\text{meq} \cdot 100\text{g}^{-1}$)	110	Titration
Basic surface FG ($\text{meq} \cdot 100\text{g}^{-1}$)	40	Titration
Mineralogy ^a	Q, S, K, C, F, G	XRD
pH	5.57	1:10 (clay : water)

pH _{ZPC}	6.4	Pot. titration
-------------------	-----	----------------

^aQ = quartz, S = smectite, K = kaolinite, C = calcite, F = feldspar and G = gypsum.

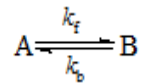
The data indicate that Cs(I) and Eu(III) retention exhibited two sorption steps: a fast initial process followed by a much slower one. The sorption occurred rapidly at the early stage of reaction was probably due to the abundant availability of active sites on resins surface. With the gradual decrease in active sites, sorption was attained at a slower rate till reaching equilibrium. The time necessary to achieve sorption equilibrium is proximity one hour and the uptake percent attained the amounts 92% and 96.3% for Cs(I) and Eu(III), respectively.

3.2.2. Kinetic modeling

The prediction of sorption rate gives important information for selecting optimum operating conditions for full-scale batch process. In order to evaluate the kinetics that control the sorption process, simple first-order, pseudo-first-order and pseudo-second-order models were used to analyze the experimental data obtained from batch experiments.

3.2.2.1. Reversible first-order model

The sorption of Cs and Eu ions from a liquid phase to a clay surface can be considered as a reversible reaction with an equilibrium state being established between two phases. Therefore, a simple first-order reaction model was used to correlate the rates of reaction, which could be expressed as:



where k_f and k_b are the forward and backward reaction rate constants. The sorption of Cs and Eu on a solid surface can be hypothesized as a reversible reaction. In this model, the relationship between fractional uptake (U) and overall rate constant (k) can be expressed as [17]:

$$\ln(1 - U) = kt \quad (5)$$

$$k = k_f + k_b \quad (6)$$

$$K_c = \frac{q_e}{C_e} = \frac{k_f}{k_b} \quad (7)$$

where k_f and k_b are the first-order rate constants for forward and backward reaction, respectively, and K_c is the equilibrium constant, C_e

is the concentration of metal ions in solution at equilibrium and q_e is the amount of metal ions adsorbed at equilibrium. Plotting the value of $\ln(1-U)$ vs. contact time (t) gives linear relations presented in Fig. 5. From these plots, the overall, forward, and backward rate constants were calculated and data are listed in Table 4. When the system reaches equilibrium the rate of forward reaction is equal to that of backward, and then the equilibrium constant, K_c , can be determined from Eq. 7. The data clarify that forward rate constant was much higher than backward rate constant for removal of both metal ions using the clay. Further, the overall rate constant and forward rate constant for Eu(III) sorption is greater than that for Cs(I) which reports the higher affinity of the applied clay to retain Eu(III) ions.

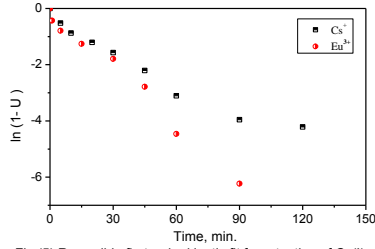


Fig.(5) Reversible first order kinetic fit for retention of Cs(I) and Eu(III) ions onto clay sample..

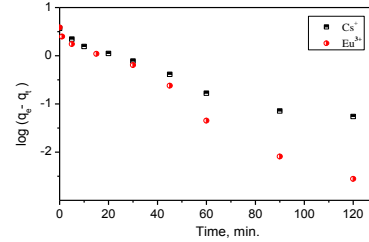


Fig.(6) Lagergren plots for retention of Cs(I) and Eu(III) ions onto clay sample.

3.2.2.2. Pseudo-first-order model

The sorption kinetic data of Cs(I) and Eu(III) retention on clay were analyzed in term of pseudo-first-order using Lagergren equation that could be written as [18]:

$$\frac{dq_t}{dt} = k_1 (q_e - q_t) \quad (8)$$

After integration and applying boundary conditions ($t = 0$ to $t = t$ and $q_t = 0$ to $q_t = q_t$) the linear form of Eq. (8) becomes:

$$\log(q_e - q_t) = \log q_e - \frac{k_1}{2.303} t \quad (9)$$

where q_t and q_e are the amounts of Cs(I) and Eu(III) adsorbed at time t and equilibrium (mg/g), respectively, and k_1 is the pseudo-first-order rate constant for the sorption process (min^{-1}). The kinetic plots of $\log(q_e - q_t)$ versus t are shown in Fig. 6. The values of q_e , k_1 and the correlation coefficients were determined from the linear plots and given in Table 4. It is evident that the correlation coefficients for the pseudo-

first-order kinetic model are relatively low and the calculated q_e values obtained from this equation do not agree with the experimental ones.

3.2.2.3. Pseudo-second-order model.

The deviation detected in fitting pseudo-first-order model had led to further verify the kinetics of Cs(I) and Eu(III) retention using pseudo-second-order rate equation that developed by Ho and McKay and expressed as [19]:

$$\frac{t}{q_t} = \frac{1}{k_2 q_e^2} + \frac{1}{q_e} t \quad (10)$$

where q_2 is the maximum sorption capacity (mg/g) for the pseudo-second-order sorption and k_2 is the equilibrium rate constant (g/mg min). The plots of t/q_t versus t for the sorption of Cs(I) and Eu(III) onto clay were drawn. From the slope and intercept values, q_2 and k_2 were calculated and the results are listed in Table 4. They were calculated to be 3.86 mg.g^{-1} and $3.95 \times 10^{-2} \text{ g.mg}^{-1}.\text{min}^{-1}$ for cesium retention on the clay while their values for europium retention were 4.01 mg.g^{-1} and $5.22 \times 10^{-2} \text{ g.mg}^{-1}.\text{min}^{-1}$, respectively.

Table 4. Kinetic parameters for retention of Cs(I) and Eu(III) ions from aqueous solution onto clay sample.

Kinetic model	Parameters	Metal ions	
		Cs	Eu
Reversible first-order	K_c	0.102	0.165
	k (min^{-1})	35.89E-3	62.43E-3
	k_f (min^{-1})	32.55E-3	56.42E-3
	k_b (min^{-1})	3.34E-3	6.01E-3
	R^2	0.946	0.984
Pseudo-first-order	k_1 (min^{-1})	35.88E-3	61.12E-3
	q_1 (mg.g^{-1})	2.37	2.90
	R^2	0.946	0.982
Pseudo-second-order	k_2 ($\text{g.mg}^{-1}.\text{min}^{-1}$)	3.95E-2	5.22E-2
	h ($\text{mg.g}^{-1}.\text{min}^{-1}$)	0.587	0.842
	q_2 (mg.g^{-1})	90.86	120.1
	R^2	0.994	0.997
Intraparticle diffusion	k_{int} ($\text{mg.g}^{-1}.\text{min}^{-0.5}$)	3.20E-1	3.22E-1
	Intercept	0.814	1.029
	R^2	0.835	0.808

The theoretical q values estimated from pseudo-second-order kinetic model for both Cs(I) and Eu(III) ions agreed with the experimental ones that had the values 3.71 and 3.85 $\text{mg}\cdot\text{g}^{-1}$, respectively. It is worth to note that, the linear plots of t/q_t versus t show a good agreement with experimental data giving the correlation coefficients close to unity. Also, the calculated q_2 values agree very well with the experimental data. This means that the sorption system fit well the pseudo-second-order kinetic for the entire sorption period, supporting the assumption that the sorption of Cs(I) and Eu(III) onto clay is mainly chemisorption and revealing that the chemical reaction was significant in the rate-controlling step [20].

3.2.2.4. Intraparticle diffusion

The pseudo-second-order kinetic model cannot give a definite mechanism of sorption. Sorption kinetics are usually controlled by different mechanisms, the most general one is the diffusion mechanism. The intraparticle diffusion model can be defined as [21]:

$$q_t = k_{\text{int}} t^{1/2} \quad (11)$$

where k_{int} is the intraparticle diffusion rate constant ($\text{mg}/\text{g}\cdot\text{min}^{1/2}$). The plot of q_t versus $t^{1/2}$ would result in a linear relationship. If the lines passed through the origin diffusion would be the controlling step. Otherwise, the intraparticle diffusion is involved in the sorption process but is not the only rate-controlling step. Some degree of boundary layer control and also other processes may be operating simultaneously to control the rate of sorption. In the case of sorption of Cs(I) and Eu(III) onto clay the plots present a multilinearity indicating that two steps are taking place. The values of constant $k_{\text{int}1}$ for intraparticle diffusion kinetics have been derived from the slopes of the linear portions and are represented in Table 4. The results indicate that the intraparticle diffusion model fits the experimental data for an initial period of the sorption process. The general features of the plots are an initial linear portion (up to 40 min) and a plateau (after 40 min). The initial linear portion is the gradual sorption stage, where intraparticle diffusion is rate controlled and the followed portion is the final equilibrium stage, where intraparticle diffusion slows down due to the low adsorbate concentration left in the solution.

Conclusion

Understanding sorption processes is fundamental for prediction of radionuclides migration in the vicinity of a disposal site of nuclear wastes. The results indicate that the applied clay has promising characteristics for application as a backfill material in disposal options. Adsorption of Cs(I) and Eu(III) is well described by pseudo second-order kinetics and the adsorption rate values exhibit the high ability of clay to immobilize such cations. Finally, the study demonstrates that, to fulfill the safety criteria, the barrier components of a disposal site need to be well characterized to predict the transport and fate of radionuclides in the surrounding environment of a nuclear waste disposal.

References

- [1] M. Y. Miah, K. Volchek, W. Kuang, F. H. Tezel, *J. Hazard. Mater.*, 183 (2010) 712–717.
- [2] S. El Mrabet, M. A. Castro, S. Hurtado, M. Mar Orta, M. C. Pazos, M. Villa-Alfageme, M. D. Alba, *Appl. Geochem.*, 40 (2014) 25–31.
- [3] M. M. Fernandes, N. Vér, B. Baeyens, *Appl. Geochem.*, 59 (2015) 189–199.
- [4] D. Li, Bo Zhang, F. Xuan, *J. Mol. Liq.*, 211 (2015) 203–209.
- [5] T. H. Wang, M. Li, S. Teng, *Appl. Radiat. Isot.*, 66 (2008) 1183–1189.
- [6] R. R. Sheha, E. A. El-Shazly, H. H. Someda, *Arab J. Nucl. Sci. Appl.*, 40(1) (2007) 127–138.
- [7] T. Shahwan, D. Akar, A.E. Eroglu, *J. Colloid Interface Sci.*, 285 (2005) 9–17.
- [8] L. Zhou, H. Zhang, M. Yan, H. Chen, M. Zhang, *Appl. Radiat. Isot.*, 82 (2013) 139–144.
- [9] M. Bouby, L. Lutzenkirchen, K. Dardenne, T. Preocanin, M.A. Denecke, R. Klenze, H. Geckeis, *J. Colloid Interface Sci.*, 350 (2010) 551–561.
- [10] N. Janot, M.F. Benedetti, P.E. Reiller, *Environ. Sci. Technol.*, 45 (2011) 5224–5230.
- [11] C.C. Ding, W.C. Cheng, Y.B. Sun, X.K. Wang, *Geochim. Cosmochim. Acta*, 165 (2015) 86–107.
- [12] Y.B. Sun, J.X. Li, X.K. Wang, *Geochim. Cosmochim. Acta*, 140 (2014) 621–643.
- [13] L. S. Clesceri, A. E. Greenberg, A. D. Eaton (Eds.), *American Water Works Association, Water Environment Federation, USA* (2000).
- [14] R. R. Sheha, *J. Colloid Interface Sci.*, 388 (2012) 21–30.

- [15] H. Jung, M.A. Malek, J. Ryu, B. Kim, Y. Song, H. Kim, C. Ro, *Anal. Chem.*, 82 (2010) 6193–6202.
- [16] C. Appel, L. Q. Ma, R. D. Rhue, E. Kennelley, *Geoderma*, 113(1–2) (2003) 77–93.
- [17] S. Rengaraj, Y. Kim, C.K. Joo, K. Choi, J. Yi, *Korean J. Chem. Eng.*, 21(1) (2004) 187–194.
- [18] R. R. Sheha, *Chem. Eng. J.*, 213 (2012) 163–174.
- [19] Y.S. Ho, G. McKay, *Water Res.*, 33 (1999) 578–584.
- [20] E. Bulut, M. Ozacar, I. A. Sengil, *J. Hazard. Mater.*, 154 (2008) 613.
- [21] M. Y. Miah, K. Volchek, W. Kuang, F. H. Tezel, *J. Hazard. Mater.*, 183 (2010) 712–717.